Synthesis of Supported Bimetal Catalysts using Galvanic Deposition Method

Yuji Mahara,[a] Junya Ohyama,[a,b] Kyoichi Sawabe,[a] and Atsushi Satsuma*[a,b]

Abstract: Supported bimetallic catalysts have been studied because of their enhanced catalytic properties due to metal–metal interactions compared with monometallic catalysts. We focused on galvanic deposition (GD) as a bimetallization method, which achieves well-defined metal–metal interfaces by exchanging heterogeneous metals with different ionisation tendencies. We have developed Ni@Ag/SiO_2 catalysts for CO oxidation, Co@Ru/Al_2O_3 catalysts for automotive three-way reactions and Pd–Co/Al_2O_3 catalysts for methane combustion by using the GD method. In all cases, the catalysts prepared by the GD method showed higher catalytic activity than the corresponding monometallic and bimetallic catalysts prepared by the conventional co-impregnation method. The GD method provides contact between noble and base metals to improve the electronic state, surface structure and reducibility of noble metals.

Yuji Mahara received his master's degree in engineering from Nagoya University in 2015. He pursued his PhD studies in Prof. Atsushi Satsuma's group at Nagoya University. His current research interests are the design of novel bimetal catalysts for automotive emission control and in situ XAFS technique.

Junya Ohyama obtained his PhD in engineering from Kyoto University in Japan in 2011. He has been a research associate at the Graduate School of Engineering, Nagoya University, Japan since 2011. His current research interests concern supported metal nanoparticle catalysts for exhaust gas purification, biomass conversion and fuel cells.

Kyoichi Sawabe received his PhD in science in 1991 from the University of Tokyo in Japan. He was a research associate at the Institute for Molecular Science and has been an assistant professor at the Graduate School of Engineering, Nagoya University, Japan since 1996. His current research interests are first principles calculation studies on catalysis and machine learning for catalyst design.

Atsushi Satsuma received his PhD in engineering in 1989 from Nagoya University in Japan. He was a research associate, an assistant professor, an associate professor and has been a professor at the Graduate School of Engineering, Nagoya University, Japan since 2003. His current research interests are in automobile catalysts and environment-friendly chemical processes.

[a] Y. Mahara, J. Ohyama, K. Sawabe, A. Satsuma
Graduate School of Engineering
Nagoya University
Furo-cho, Nagoya 464-8603 (Japan)
E-mail: satsuma@chembio.nagoya-u.ac.jp

[b] J. Ohyama, A. Satsuma
Elements Strategy Initiative for Catalysts and Batteries (ESICB)
Kyoto University
Katsura, Kyoto 615-8520 (Japan)

1. Introduction

The design and synthesis of novel supported metal catalysts is a crucial theme for sustainable chemistry and efficient energy conversion. Supported platinum group metal (PGM) catalysts are used as environmental catalysts to purify exhaust gases from automobiles and factories.[1] However, PGMs are expensive and rare. From an elemental viewpoint, a reduction in PGM usage or the development of alternative catalysts are desired.

Catalytic activity and selectivity are often promoted by combining two different metals because of metal–metal interactions. Metal–metal interactions modify catalytic properties via several factors: (1) the ligand effect, where changes in the electronic state of metal surfaces influence the reactivity of the catalyst;[2] (2) the ensemble effect, where the unique geometric structure of bimetallic catalysts allows/forbids the progress of catalytic reactions;[3] (3) the strain effect, where disorder in the atomic arrangement due to the mismatching of lattice constants changes the catalytic activity.[4]

Finding alternatives to PGMs that contain only base metal is an arduous task, and the most practical method is to combine a noble and a base metal. The structure of the bimetallic catalyst is classified into a solid solution, core shell, and Janus (phase separation type).[5] A closer contact between heterogeneous metals leads to stronger metal–metal interaction. Ultimately, the electronic state may drastically change in the solid solution (alloy) form. However, many substitutional alloys of noble and base metals are unstable because of the mismatching of their lattice constants and crystal structures. For example, with respect to alloys of Ag and base metals, Ag–Co and Ag–Ni are immiscible combinations.[6] Similarly, Ru–Co, Ru–Cu and Ru–Ni are immiscible because of the differences in crystal structure.[7] In the case of Pd, even when Pd–M (M: V, Mn, Fe, Co, Ni, Zn, Sn) is synthesised as alloy particles, phase separation occurs depending on the temperature and gaseous atmosphere.[8] Therefore, the advance preparation of stable and highly active catalysts with a phase-separated structure (core shell or Janus) is reasonable.

By using the conventional co-impregnation and co-precipitation method, two metals can be mixed; however, at the same time, a single metal particle can be produced independently.[8a, 9] In the sequential impregnation method, a metal (M_1) is loaded on a support, and another metal (M_2) is supported thereon. By using this method, it is not possible to control whether M_2 is formed on M_1 or the support.[9] In the liquid phase reduction method using organic ligands, even if the catalyst structure can be controlled well, an organic ligand such as PVP causes catalyst poisoning and poor atomic efficiency.[10]

Galvanic deposition (GD) is a useful method for making a bimetallic catalyst with a unique metal–metal interface. Scheme 1 shows an overview of the GD method. With the GD method, a metal (M_1) having a high ionisation tendency is previously reduced and supported, and a solution that contains ions of another metal (M_2) with a relatively low ionisation tendency is dropped thereon, whereby M_2 is stabilised on M_1 according to the following formula:

$$nM_1^0 + mM_2^{n+} \rightarrow nM_1^{m+} + mM_2^0.$$

As a result, the M_2 monolayer, which provides good active sites, ideally precipitates on M_1 particles. Thereafter, the underlying metal is eroded by the additive metal, thus exposing a unique surface, and the added metal is deposited on this surface. This contact could cause higher strain and stronger metal–metal interactions than in the case of bimetallization among stable phases. The GD method has attracted attention as a method of preparing electrode catalysts for fuel cells.[11] In recent years, it has been applied to a wide range of reactions such as hydrogenation,[12] oxidation[13] and selective reduction.[14]

We applied the GD method to various combinations of metals and developed Ni@Ag/SiO_2 catalysts[15] for CO oxidation, Co@Ru/Al_2O_3 catalysts[16] for three-way automotive reactions and Pd–Co/Al_2O_3 catalysts[17] for methane combustion. This personal account gives an outline of these studies and describes the strategy of using bimetallic catalysts to replace PGM catalysts.

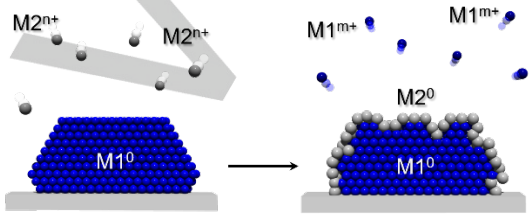

Scheme 1. Illustration of GD method.

2. Ni@Ag core-shell catalysts for CO oxidation

In this section, we report the synthesis of an automotive catalyst that contains only non-platinum group elements. This is a challenging problem and a drastic change in the catalytic properties of the base metal is desired. CO oxidation is the most studied model reaction in exhaust gas purification. In this reaction, sub-nanoparticles of d_{10} metals such as Au or Ag show surprisingly high activity at low temperatures.[18] This is due to the quantum size effect, which is expressed when the d_{10} metal is in a sub-nanosized form. Moreover, DFT calculations predict that bimetallization causes a change in the electronic properties of the metal. However, Ag and 3*d* transition metals such as Ni, Co and Fe are combinations that do not form a solid solution thermodynamically, and it is impossible to make such alloy nanoparticles.[6c] (A few studies describe the formation of Ag–Ni alloy nanoparticles by using a special method, *i.e.* γ irradiation.[6c]) We precipitated Ag on the Ni nanoparticles of Ni/SiO_2 by using the GD method to produce a partial Ag–Ni alloy structure. In conclusion, we successfully synthesised Ni@Ag/SiO_2 catalysts with high CO oxidation activity.

2.1. Synthesis and CO oxidation properties

Ag–Ni/SiO_2 bimetallic catalysts were prepared using the GD method as shown in previous reports.[15] Briefly, a silica-supported Ni catalyst (Ni/SiO_2) with a 5 wt% Ni loading was prepared by the conventional impregnation method. After reducing the Ni/SiO_2 with H_2 at 400 °C, degassed water and an ethanol solution of $AgNO_3$ were injected into the Ni^0/SiO_2 at 298 K. The Ag–Ni/SiO_2

catalysts were gained after centrifugation and drying (denoted as AgNi-GD298).

Figure 1(a–d) show a high-angle annular dark-field scanning transmission electron microscopy (HAADF-STEM) image and an energy dispersive X-ray (EDX) elemental map of AgNi-GD298 after CO oxidation. Ni, shown in red, and Ag, shown in green, certainly co-exist, thus indicating that the GD reaction proceeded successfully. However, there was limited contact between Ag and Ni because Ag was present in the form of particles. In this situation, the contribution from alloying was small. Agglomeration of Ag to particles was due to temperature during galvanic replacement. Even at room temperature, Ag can aggregate by heat and light. Therefore, to improve the catalyst preparation, a catalyst was newly prepared by the GD method at 213 K (denoted AgNi-GD213). Figs. 1(e–h) show the STEM images and EDX elemental maps of AgNi-GD213. These were significantly different from AgNi-GD298, and Ag was evenly distributed on Ni. In AgNi-GD213, comparatively small Ag particles were observed. Figs. 1(g, h) show enlarged images of the yellow square in Fig. 1(e). Ag formed a shell structure covering the Ni particles. To determine the coordination number (CN) of Ag in the prepared catalysts, Ag K-edge X-ray absorption fine structure (XAFS) measurements were conducted as shown in Fig. 1(i). The CN of the Ag–Ag bond in AgNi-GD213 is smaller than in AgNi-GD298, and Ag is considered to spread as a thin shell or highly dispersed nanoparticles. The loading amounts of Ag and Ni on AgNi-GD213 measured by ICP were 0.3 wt% Ag and 3 wt% Ni. For comparison, $Ag(0.3)/SiO_2$ and $Ni(3)/SiO_2$ were prepared by the impregnation method as reference catalysts for the activity tests (metal loading in parenthesis). Pd/SiO_2, which shows high activity for CO oxidation, was also prepared ($Pd(5)/SiO_2$).

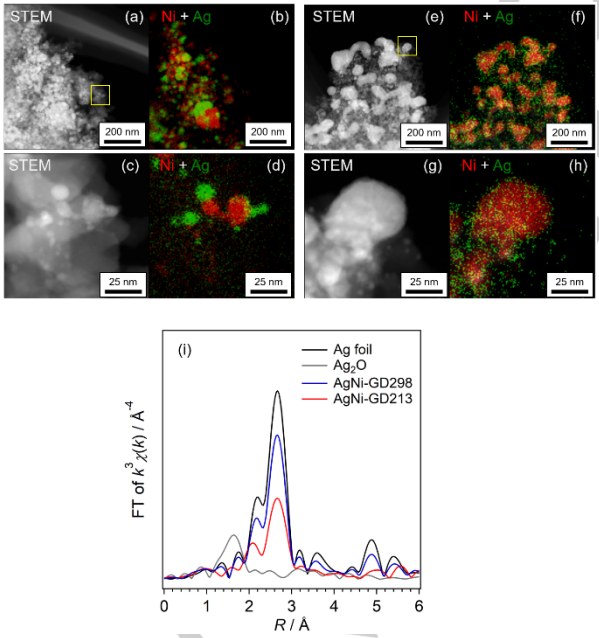

Fig. 1. HAADF-STEM image and EDX elemental maps of (a–d) AgNi-GD298 and (e–h) AgNi-GD213 after use for CO oxidation. (c, d, g, h) are enlarged views of the yellow square in Fig. 1(a, e), respectively. For the elemental maps, Ag is indicated in green, Ni in red and Ag+Ni in yellow. (i) FT of k^3-weighted Ag K-edge EXAFS spectra of Ag foil, Ag_2O, AgNi-GD298 and AgNi-GD213. The samples were measured after use for CO oxidation.

Figure 2(a) shows the results of activity tests for CO oxidation. Although $Ni(3)/SiO_2$ alone has no activity below 200 °C, CO oxidation over AgNi-GD213 proceeded at approximately 50 °C lower than over $Ag(0.3)/SiO_2$. In the low-temperature range, AgNi-GD213 showed higher catalytic activity than $Pd(5)/SiO_2$.

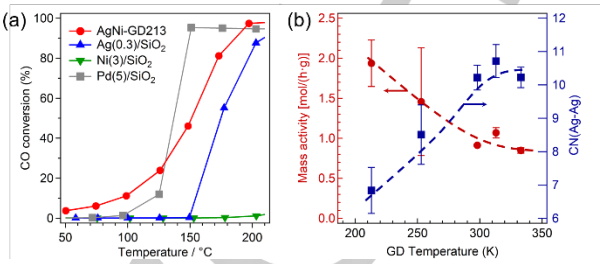

Fig. 2. (a) CO conversion over AgNi-GD213 (red), $Ag(0.3)/SiO_2$ (blue), $Ni(3)/SiO_2$ (green) and $Pd(5)/SiO_2$ (grey). (b) Variation of the mass activity of CO oxidation and the CN of Ag–Ag with temperature for the GD catalyst preparation reaction.

To examine the effect of temperature on the GD reaction in detail, we prepared catalysts for which the temperature of the GD reaction was changed from 213 K to 333 K. Table 1 shows the curve-fitting result of Ag K-edge extended XAFS (EXAFS) for a series of AgNi-GD catalysts. A decrease in the CN of Ag–Ag and the distance of the Ag–Ag bond were observed with a decrease in the preparation temperature. The mass activity per Ag for CO oxidation at 100 °C by using the catalysts was evaluated. Additionally, the CN of the Ag–Ag bond in the catalyst after CO oxidation was calculated from Ag K-edge XAFS measurements. The results are shown in Fig. 2(b). A lower temperature of the GD reaction for the catalysts corresponds to the higher mass activity of CO oxidation and the lower CN of Ag–Ag. At a lower GD temperature, Ag forms smaller particles on Ni and can exist as a thin shell or island (see Fig. 1). Therefore, owing to the closer contact with Ni, the electronic state of Ag should be changed to improve the CO oxidation activity.

3. Co@Ru core-shell catalysts for three-way reactions

In automotive catalysts for gasoline-fuelled engines, Rh is indispensable because of its high NOx reducing ability.[19] However, Rh is a valuable element and it has lower reserves than other metals. The substitution of Rh with other base metals is meaningful from the view of not only the chemical industry but also new science. Ru is one of the most promising alternatives to Rh. Although Ru is a platinum group element, it is much cheaper than Rh. We first attempted to develop an alternative to Rh catalysts by changing the properties of Ru by bimetallization with a 3*d* transition metal.

3.1 Synthesis and characterisation

Alumina-supported Co@Ru core-shell catalysts were synthesised by the GD method according to a procedure in the literature (Co@Ru-GD).[16] As references, Ru/Al_2O_3 and Co/Al_2O_3 were prepared by the conventional impregnation method (Ru-imp and Co-imp). $Ru/Co/Al_2O_3$ was prepared by the sequential impregnation method (Ru/Co-seq). The HAADF-STEM image and EDX elemental maps indicate that the Ru species of Co@Ru-GD exists in the overlapping region (Fig. 3(a)). It is expected that Ru and Co are alloyed, or either Ru or Co is on one of them. On the contrary, in Ru/Co-seq, Ru and Co only partially overlapped and mostly existed as separate metals (Fig. 3(b)). We observed the FT-IR spectrum of adsorbed CO after reduction at 500 °C (CO adsorption FT-IR). In all samples including Ru, intense bands derived from CO on Ru could be observed, thus suggesting that Ru in Co@Ru-GD was exposed on the surface (Fig. 3(c)). From the Fourier transformed Ru K-edge EXAFS spectrum of Co@Ru-GD after reduction at 500 °C, a peak derived from Ru–Ru bonds was confirmed (Fig. 3(d)). Therefore, it is understood that the Ru–Co alloy is not the main structure. The results of STEM/EDX, CO adsorption FT-IR and Ru K-edge EXAFS indicate that Co@Ru-GD has a core-shell structure in which Ru is the shell and Co is the core, as shown in Fig. 3(e). By contrast, Ru/Co-seq has the structure shown in Fig. 3(f), in which the Ru and CoO_x phases are separated.

Table 1. Curve-fitting results for the k^3-weighted Ag K-edge EXAFS data for a series of AgNi catalysts.

Catalysts	CN(Ag–Ag)	*R*(Ag–Ag)/Å	σ^2/Å^2	R_f /%
AgNi-213GD	6.8 ± 0.5	2.84 ± 0.01	0.0119 ± 0.0004	0.1
AgNi-253GD	8.5 ± 1.8	2.85 ± 0.01	0.0136 ± 0.0016	2.0
AgNi-298GD	10.2 ± 0.7	2.86 ± 0.003	0.0107 ± 0.0005	0.2
AgNi-313GD	10.7 ± 1.0	2.86 ± 0.003	0.0107 ± 0.0005	0.2
AgNi-333GD	10.2 ± 0.6	2.86 ± 0.003	0.0106 ± 0.0004	0.1

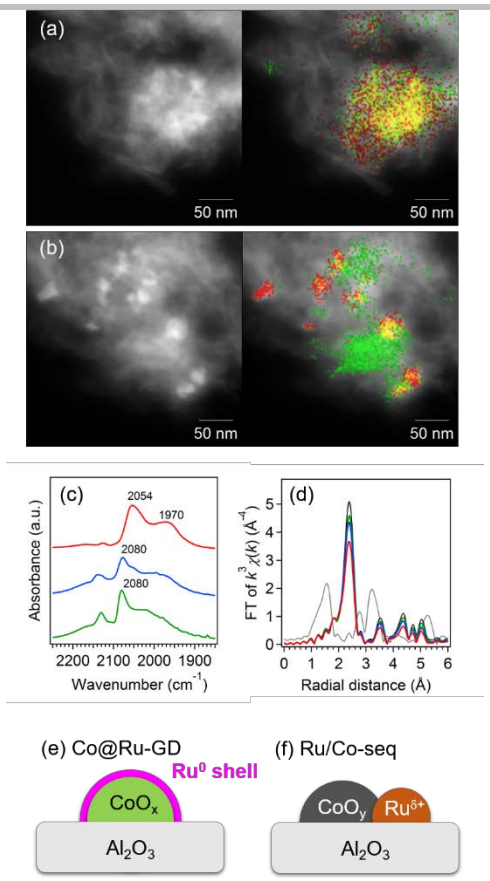

Fig. 3. Typical HAADF-STEM images and those overlaid with Ru and Co EDS elemental maps for (a) Co@Ru-GD and (b) Ru/Co-seq. For the elemental maps, Ru is indicated in red, Co in green and Ru+Co in yellow. (c) CO adsorption FT-IR spectra of Co@Ru-GD (red), Ru/Co-seq (blue) and Ru-imp (green). (d) FT of k^3 weighted Ru K-edge EXAFS spectra of Co@Ru-GD (red), Ru/Co-seq (blue), Ru-imp (green), Ru metal powder (black) and RuO_2 (grey). Schematic drawings of the structures of (e) Co@Ru-GD and (f) Ru/Co-seq.

In the CO adsorption FT-IR of Ru-imp and Ru/Co-seq, the intense band at ca 2080 cm^{-1} is attributed to the CO adsorbed on low-coordination Ru sites (Fig. 3(c)). However, the adsorption band of CO on the Ru in Co@Ru-GD was different from that for other catalysts. The band at 2054 cm^{-1} is assigned to linearly adsorbed CO species atop Ru atoms on Ru terrace sites, and the band at 1970 cm^{-1} is assigned to bridge-bonded CO. These results suggest that terrace surfaces with large Ru particles appear because Ru is a core-shell structure covering CoO_x.

3.2 Automotive three-way reaction

The catalytic activity of the NO-C_3H_6-CO-O_2 reaction (the automotive three-way reaction) was measured with a conventional fixed-bed flow reactor at atmospheric pressure. The reaction gases including 1,000 ppm of NO, 4,000 ppm of CO, 1,000 ppm of propylene (C_3H_6), 6,000 ppm of O_2 and the balance Ar passed through 17.5 mg of the prepared catalyst in a stoichiometric ratio (GHSV = 140,000 h^{-1}).

Figure 4 shows (a) NO, (b) C_3H_6 and (c) CO conversions over the prepared catalysts as a function of reaction temperature. The conversion of NO on Co@Ru-GD progressed at approximately 50 °C lower than on Ru/Co-seq and Ru-imp. The NO conversion in this reaction is consistent with that in the NO–C_3H_6 reaction, which is not consistent with that in the NO–CO reaction (there is no data; see previous paper). Therefore, NO reacts with C_3H_6 on the catalyst surface. In various papers, it is reported that the rate-limiting step of this reaction over the platinum metal catalysts is the reduction of metal oxide with CO or C_3H_6. A high NO conversion activity with Co@Ru-GD can be achieved by improving the reducibility of Ru.

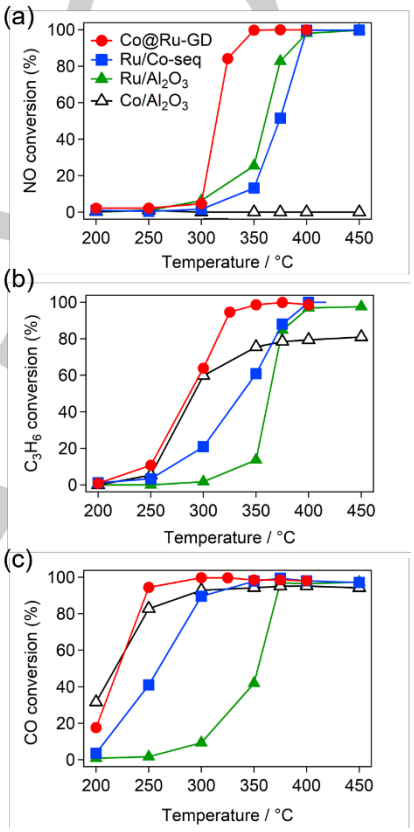

Fig. 4. (a) NO, (b) C_3H_6 and (c) CO conversions as a function of reaction temperature for the NO–C_3H_6–CO–O_2 reaction over Co@Ru-GD (red circle), Ru/Co-seq (blue square), Ru-imp (green triangle) and Co-imp (black open triangle).

To investigate the oxidation/electronic state of the Ru surface, Ru X-ray photoelectron spectroscopy (XPS) was performed after reduction with H_2 at 500 °C. The peak derived from Ru 3d shifted to low energy because of the electron transfer between the Ru and Co species on Co@Ru-GD (Fig. 5(a)). C_3H_6 temperature programmed reduction (C_3H_6-TPR) was conducted to investigate the reducibility of Ru oxide by C_3H_6 (Fig. 5(b)). Over Co@Ru-GD, the reduction by C_3H_6 progressed at a lower temperature than over Ru/Co-seq and Ru-imp. To summarise the above, when a Co-Ru core-shell structure was prepared by the GD method, the electronic state of Ru changed because of the formation of a shell on Ru on Co. The RuO_x species oxidised from such Ru shells were highly active in the low-temperature range for the NO–

C_3H_6–CO–O_2 reaction because they are reduced from the low-temperature state by C_3H_6.

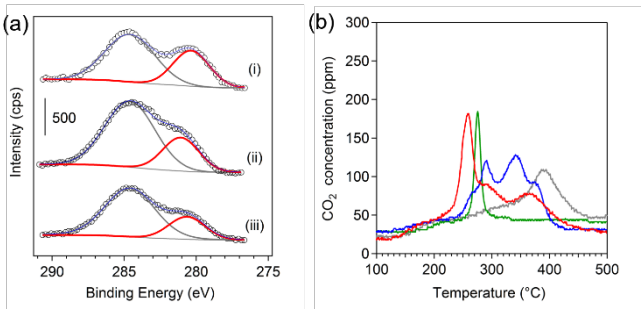

Fig. 5. (a) Ru 3d XPS of (i) Co@Ru-GD, (ii) Ru/Co-seq and (iii) Ru-imp. The raw data are indicated by open circles. The spectra were deconvoluted with two curves: Ru $3d_{5/2}$ XPS in red and the mixture of C1s and Ru $3d_{3/2}$ in grey. (b) C_3H_6-TPR of Co@Ru-GD (red solid), Ru/Co-seq (blue), Ru-imp (green) and Co-imp (grey).

4. Pd–Co/Al_2O_3 catalysts for methane combustion

A supported Pd catalyst is a useful automotive catalyst because of its high hydrocarbon oxidising ability. Methane is the most stable component among the hydrocarbons, and this gas is difficult to burn completely. The complete combustion of methane using a supported Pd catalyst is important for automobiles and thermal power generation. To reduce the amount of Pd used, further development of a highly active Pd catalyst is desired. In methane combustion, the redox ability of Pd is a key factor. We aimed to develop a catalyst exhibiting high methane combustion activity by combining Pd with a 3d transition metal oxide via the GD method.

4.1 Synthesis and characterisation

Pd–Co/Al_2O_3 was prepared according to a procedure described in a previous paper (PdCo-GD).[17] As a reference, Pd/Al_2O_3 and Co/Al_2O_3 were prepared by the conventional impregnation method (Pd-imp and Co-imp). Pd/Co/Al_2O_3 was prepared by the sequential impregnation method (PdCo-seq). Figs. 6(a–c) show the STEM/EDX images of PdCo-GD. Pd existed as particles with a size of 5–10 nm. Co was dispersed on Al_2O_3, and the EDX elemental maps of Pd and Co overlapped. With this result alone, it is impossible to determine whether Pd and Co form an alloy or are phase-separated. Therefore, Pd and Co K-edge XAFS spectra were recorded to investigate the surrounding structure of the metal in the catalyst after the reaction. From Fourier transform EXAFS, Pd–O, Pd–Pd and Pd–O bond peaks derived from the PdO structure were observed for Pd, and a Co–Co bond peak derived from highly dispersed Co_3O_4 was observed for Co (Fig. 6(d)). From the results of STEM/EDX and XAFS, it was found that PdO nanoparticles and the CoO_x dispersed particles of PdCo-GD existed nearby, as shown in Fig. 6(e).

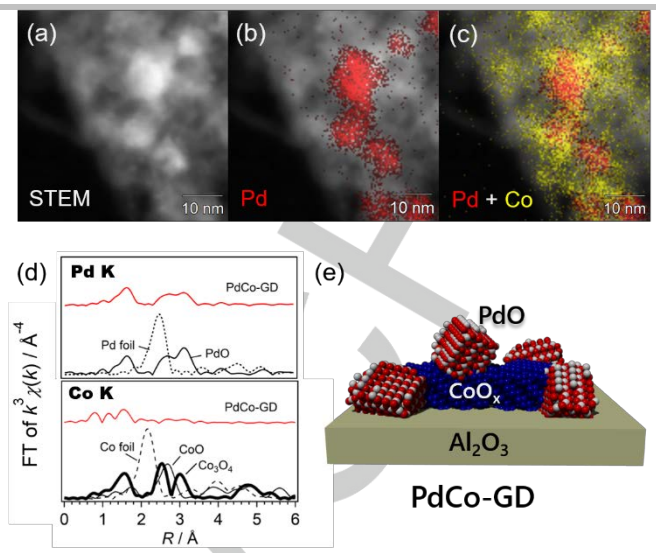

Fig. 6. (a) HAADF-STEM image and (b, c) EDX elemental maps of PdCo-GD. The red and yellow areas in EDX correspond to Pd and Co, respectively. (d) FT of k^3-weighted Pd K-edge and Co K-edge EXAFS spectra of PdCo-GD after use for methane combustion. (e) Schematic illustration of PdCo-GD.

4.2 Methane combustion

Catalytic tests of methane combustion were performed with a conventional fixed-bed flow reactor at atmospheric pressure with 20 mg of catalyst in a Pyrex glass tube with an internal diameter of 4 nm. After pre-treatment involving oxidation and reduction at 500 °C, 0.4 vol% CH_4/10 vol% O_2/N_2 balance at a rate of 100 mL/min were passed through the catalyst (lean burn conditions). A temperature between 200 and 600 °C was held for 30 min, and the CH_4 conversion was measured.

Figure 7(a) shows the results of catalytic tests. The light-off of methane combustion over PdCo-GD progressed at approximately 50 °C lower than over Pd-imp. On the other hand, PdCo-seq had a lower activity than Pd-imp. This is because the size of Pd supported by the conventional sequential impregnation method is extremely small. To dissociate the C–H bond of methane, a moderate PdO ensemble is necessary; in PdCo-seq, there were fewer PdO ensembles for methane dissociation. Even though PdCo-GD and Pd-imp have almost the same sized Pd particles, the catalytic activity differs significantly. For methane combustion on Pd-based catalysts, the redox properties of Pd are key to the high activity.[20] O_2-temperature programmed desorption (O_2-TPD) was used to evaluate the reducibility of PdO in the catalysts. PdO in PdCo-GD released O at a lower temperature than in other catalysts (Fig. 7(b)). Considering the catalyst structure, O probably escapes at the interface between PdO particles and Co_3O_4 (or PdO particles on Co_3O_4), and the redox properties of the PdO species are improved. The activity of PdCo-GD for methane combustion is enhanced because of this improvement.

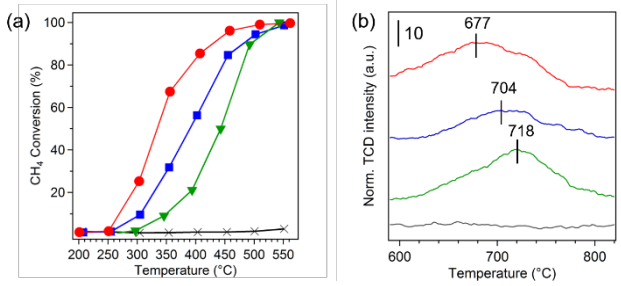

Fig. 7. (a) Methane combustion over PdCo-GD (red circle), Pd-imp (blue square), PdCo-seq (green triangle) and Co-imp (black cross). (b) O_2-TPD of PdCo-GD (red), Pd-imp (blue), PdCo-seq (green) and Co-imp (grey).

5. Summary and prospects

GD provided an effective preparation method for bimetallic catalysts for automotive catalytic reactions. By using the GD method, Ni@Ag/SiO_2 (Section 2) for CO oxidation, Co@Ru/Al_2O_3 (Section 3) for the NO–C_3H_6–CO–O_2 reaction and PdCo/Al_2O_3 (Section 4) for methane combustion were developed. In all cases, the metal–metal and metal–metal oxide interfaces resulted in a change in the catalytic properties. The morphology of the Ag–Ni catalyst was greatly affected by the temperature of the GD reaction, and the Ni–Ag core-shell structure formed below −60 °C. The GD method enabled contact even with metal combinations that are immiscible in nature (i.e. Ag–Ni). In the Ru–Co system, abundant Ru terraces appeared adjacent to the CoO_x, and the redox ability of RuO_x improved. Likewise, the Pd–Co system improved the redox properties of the PdO species by the contact between the CoO_x and PdO particles. The GD method is an attractive preparation method that requires no special organic protective agents or polymers but only hydrogen gas. These advantages will allow it to be used in the future as a catalyst preparation method for various reactions.

Acknowledgements

This work was supported by Grant-in-Aids from the Ministry of Education, Culture, Sports, Science and Technology (MEXT), Japan, Elements Strategy Initiative to Form Core Research Center program (ESICB), Grants-in-Aid for Scientific Research KAKENHI (B) (15H04186) and Research Fellowships of Japan Society for the Promotion of Science for young Scientists (JSPS).

REFERENCES

[1] H. Hirata, *Catal. Surv. Asia* **2014**, *18*, 128-133.

[2] aJ. Greeley, J. K. Nørskov, *Surf. Sci.* **2005**, *592*, 104-111; bJ. Zhang, H. Jin, M. B. Sullivan, F. C. Lim, P. Wu, *Phys. Chem. Chem. Phys.* **2009**, *11*, 1441-1446; cS. Xie, S. I. Choi, N. Lu, L. T. Roling, J. A. Herron, L. Zhang, J. Park, J. Wang, M. J. Kim, Z. Xie, M. Mavrikakis, Y. Xia, *Nano Lett.* **2014**, *14*, 3570-3576.

[3] aM. S. Chen, D. W. Goodman, *Science* **2004**, *306*, 252-255; bF. Gao, D. W. Goodman, *Chem. Soc. Rev.* **2012**, *41*, 8009-8020; cH. Miura, K. Endo, R. Ogawa, T. Shishido, *ACS Catal.* **2017**, *7*, 1543-1553.

[4] M. Mavrikakis, B. Hammer, J. K. Nørskov, *Phys. Rev. Lett.* **1998**, *81*, 2819.

[5] R. Ferrando, J. Jellinek, R. L. Johnston, *Chem. Rev.* **2008**, *108*, 845-910.

[6] aA. Holewinski, J. C. Idrobo, S. Linic, *Nat. Chem.* **2014**, *6*, 828-834; bZ. Zhang, T. M. Nenoff, J. Y. Huang, D. T. Berry, P. P. Provencio, *J. Phys. Chem. C* **2009**, *113*, 1155-1159; cZ. Zhang, T. M. Nenoff, K. Leung, S. R. Ferreira, J. Y. Huang, D. T. Berry, P. P. Provencio, R. Stumpf, *J. Phys. Chem. C* **2010**.

[7] aM. Cerro-Alarcón, A. Maroto-Valiente, I. Rodríguez-Ramos, A. Guerrero-Ruiz, *Appl. Catal., A* **2004**, *275*, 257-269; bX. He, S.-H. Liang, J.-H. Li, B.-X. Liu, *Phys. Rev. B* **2007**, *75*.

[8] aK. Persson, A. Ersson, K. Jansson, N. Iverlund, S. Jaras, *J. Catal.* **2005**, *231*, 139-150; bJ. J. Willis, E. D. Goodman, L. Wu, A. R. Riscoe, P. Martins, C. J. Tassone, M. Cargnello, *J. Am. Chem. Soc.* **2017**, *139*, 11989-11997.

[9] aA. Satsuma, T. Tojo, K. Okuda, Y. Yamamoto, S. Arai, J. Oyama, *Catal. Today* **2015**, *242*, 308-314; bP. Stefanov, S. Todorova, A. Naydenov, B. Tzaneva, H. Kolev, G. Atanasova, D. Stoyanova, Y. Karakirova, K. Aleksieva, *Chem. Eng. J.* **2015**, *266*, 329-338.

[10] aN. Toshima, T. Yonezawa, *New J. Chem.* **1998**, *22*, 1179-1201; bL. Xia, X. Hu, X. Kang, H. Zhao, M. Sun, X. Cihen, *Colloids Surf., A* **2010**, *367*, 96-101; cJ. P. Holgado, F. Ternero, V. M. Gonzalez-delaCruz, A. Caballero, *ACS Catal.* **2013**, *3*, 2169-2180; dJ. Xiang, P. Li, H. Chong, L. Feng, F. Fu, Z. Wang, S. Zhang, M. Zhu, *Nano Res.* **2014**, *7*, 1337-1343.

[11] aJ. Zhang, M. B. Vukmirovic, Y. Xu, M. Mavrikakis, R. R. Adzic, *Angew. Chem. Int. Ed.* **2005**, *44*, 2132-2135; bS. W. Price, J. D. Speed, P. Kannan, A. E. Russell, *J. Am. Chem. Soc.* **2011**, *133*, 19448-19458; cS. Papadimitriou, S. Armyanov, E. Valova, A. Hubin, O. Steenhaut, E. Pavlidou, G. Kokkinidis, S. Sotiropoulos, *J. Phys. Chem. C* **2010**, *114*, 5217-5223; dY. Lu, S. Du, R. Steinberger-Wilckens, *Appl. Catal., B* **2016**, *199*, 292-314; eM. Shao, P. Liu, J. Zhang, R. Adzic, *J. Phys. Chem. B* **2007**, *111*, 6772-6775; fM. Wang, W. Zhang, J. Wang, D. Wexler, S. D. Poynton, R. C. Slade, H. Liu, B. Winther-Jensen, R. Kerr, D. Shi, J. Chen, *ACS Appl. Mater. Interfaces* **2013**, *5*, 12708-12715; gB. Lim, M. Jiang, P. H. Camargo, E. C. Cho, J. Tao, X. Lu, Y. Zhu, Y. Xia, *Science* **2009**, *324*, 1302-1305; hI. Mintsouli, J. Georgieva, E. Valova, S. Armyanov, A. Kakaroglou, A. Hubin, O. Steenhaut, J. Dille, A. Papaderakis, G. Kokkinidis, S. Sotiropoulos, *J. Solid State Electrochem.* **2012**, *17*, 435-443; iJ. Son, S. Cho, C. Lee, Y. Lee, J. H. Shim, *Langmuir* **2014**, *30*, 3579-3588; jM. Shao, K. Sasaki, N. Marinkovic, L. Zhang, R. Adzic, *Electrochem. Commun.* **2007**, *9*, 2848-2853; kH. Zhang, M. Jin, J. Wang, W. Li, P. H. Camargo, M. J. Kim, D. Yang, Z. Xie, Y. Xia, *J. Am. Chem. Soc.* **2011**, *133*, 6078-6089.

[12] aL. Zhu, H. Sun, J. Zheng, C. Yu, N. Zhang, Q. Shu, B. H. Chen, *Mater. Chem. Phys.* **2017**, *192*, 8-16; bL. Zhu, T. Zheng, C. Yu, J. Zheng, Z. Tang, N. Zhang, Q. Shu, B. H. Chen, *Appl. Surf. Sci.* **2017**, *409*, 29-34; cT. Kim, X. Fu, D. Warther, M. J. Sailor, *ACS Nano* **2017**, *11*, 2773-2784; dY. Wu, D. Wang, G. Zhou, R. Yu, C. Chen, Y. Li, *J. Am. Chem. Soc.* **2014**, *136*, 11594-11597; eT. Yoshii, K. Nakatsuka, Y. Kuwahara, K. Mori, H. Y. Hiromi Yamashita, *RSC Adv.* **2017**, *7*, 22294-22300.

[13] X. Pan, Y. Zhang, Z. Miao, X. Yang, *J. Energy Chem.* **2013**, *22*, 610-616.

[14] aJ.-H. Kim, H. Woo, S.-W. Yun, H.-W. Jung, S. Back, Y. Jung, Y.-T. Kim, *Appl. Catal., B* **2017**, *213*, 211-215; bY. Zhang, W. Diao, J. R. Monnier, C. T. Williams, *Catal. Sci. Technol.* **2015**, *5*, 4123-4132.

[15] aY. Mahara, H. Ishikawa, J. Ohyama, K. Sawabe, A. Satsuma, *Catal. Today* **2016**, *265*, 2-6; bY. Mahara, H. Ishikawa, J. Ohyama, K. Sawabe, Y. Yamamoto, S. Arai, A. Satsuma, *Chem. Lett.* **2014**, *43*, 910-912.

[16] J. Ohyama, H. Ishikawa, Y. Mahara, T. Nishiyama, A. Satsuma, *Bull. Chem. Soc. Jpn.* **2016**, *89*, 914-921.

[17] Y. Mahara, J. Ohyama, T. Tojo, K. Murata, H. Ishikawa, A. Satsuma, *Catal. Sci. Technol.* **2016**, *6*, 4773-4776.

[18] aM. Haruta, T. Kobayashi, H. Sano, N. Yamada, *Chem. Lett.* **1987**, *16*, 405-408; bM. Haruta, *Chem. Rec.* **2003**, *3*, 75-87; cK. i. Shimizu, K. Sawabe, A. Satsuma, *ChemCatChem* **2011**, *3*, 1290-1293.

[19] P. Granger, V. I. Parvulescu, *Chem. Rev.* **2011**, *111*, 3155-3207.

[20] aP. Castellazzi, G. Groppi, P. Forzatti, A. Baylet, P. Marécot, D. Duprez, *Catal. Today* **2010**, *155*, 18-26; bY.-H. Chin, M. García-Diéguez, E. Iglesia, *J. Phys. Chem. C* **2016**, *120*, 1446-1460; cS. Colussi, A. Trovarelli, E. Vesselli, A. Baraldi, G. Comelli, G. Groppi, J. Llorca, *Appl. Catal., A* **2010**, *390*, 1-10.

Entry for the Table of Contents (Please choose one layout)

Layout 1:

PERSONAL ACCOUNT

Galvanic deposition (GD) is a method for preparing bimetal catalysts that have strong metal–metal interactions. In this account, we outline the development of environmental catalysts prepared by the GD method.

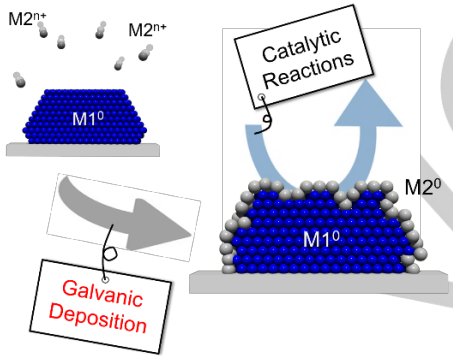

*Author(s), Corresponding Author(s)**

Page No. – Page No.

Title